Orbital ordering in $La_{0.5}Sr_{1.5}MnO_4$: Density functional and exact diagonalization studies

K. V. Shanavas* and S. Satpathy
Department of Physics & Astronomy, University of Missouri, Columbia, Missouri 65211, USA
(Received 9 April 2013; published 27 June 2013)

The nature of orbital ordering and type of the Jahn-Teller (JT) distortion in the doped manganite $La_{0.5}Sr_{1.5}MnO_4$ has been a topic of long standing debate, with both experiments and theory supporting opposite views. With the help of *ab initio* density functional and exact diagonalization studies we have investigated the energetics of the cooperative JT distortion and orbital ordering in this system. The density functional calculations yield a $x^2 - 1/y^2 - 1$ (rod-type) orbital order as well as a Jahn-Teller distortion where the octahedral axes on the plane are elongated along the chain direction and compressed perpendicular to it in the *ab* plane (type I). The essential physics of the problem is captured by a single zigzag chain model, which was studied with a tight-binding Hamiltonian and exact diagonalization on a finite chain, which help unravel the reason for the rod-type orbital order. The main conclusions from the latter studies are that: (i) The Coulomb correlation effects are relatively unimportant due to the low electron density in the e_g states, (ii) the kinetic energy term (hopping along the ferromagnetic zigzag chain) favors the rod-type orbital order, and (iii) a significant noncubic crystal field, proposed earlier and found here from our DFT calculations, helps stabilize the rod-type orbital order even further.

DOI: 10.1103/PhysRevB.87.235137 PACS number(s): 71.27.+a, 71.70.Ch, 71.10.−w, 71.70.Ej

I. INTRODUCTION

Transition metal atoms such as Mn or Cu may become Jahn-Teller active in crystalline oxides if the degenerate e_g states of these ions are singly occupied. The materials then exhibit a complex interplay between spin, charge, orbital, and lattice degrees of freedom which manifests in unusual physical properties such as high temperature superconductivity, colossal magnetoresistance, and magnetostructural transitions.[1,2] The layered manganite $La_{1-x}Sr_{1+x}MnO_4$ is an example of such competition,[3] which for commensurate doping levels (i.e., $x = \frac{1}{2}$) forms an insulating phase with crystallographically equivalent Mn sites, with an average valency of 3.5 at room temperature. Upon cooling, it displays a phase transition at ≈240 K, below which charge ordering makes the Mn sites inequivalent with a checkerboard arrangement of Mn^{3+} and Mn^{4+} sites.[4] Presence of strong Hund's coupling and cubic crystal field means that three of the four electrons (d^4) at the Mn^{3+} site goes to the three $t_{2g\uparrow}$ levels (3/2 core moment) and one to the degenerate $e_{g\uparrow}$. The system can gain energy by lifting the degeneracy of the e_g levels through cooperative JT distortions of the surrounding oxygen octahedra, which has been observed experimentally.[3,5] At further lower temperatures ($T_N \approx 110$ K) magnetic order develops in which Mn spins form ferromagnetic zigzag chains on the *ab* plane, coupled antiferromagnetically to each other, known as the CE phase.[4]

However, the type of orbital order and JT distortion present in $La_{0.5}Sr_{1.5}MnO_4$ is still a matter of considerable debate. The bridge site atom is nominally Mn^{3+} and is therefore expected to be a JT ion (labeled A in Fig. 1), while the corner site atom (labeled B in the same figure) is not JT active because of its nominal chemical valence of Mn^{4+}. In one of the earliest studies, using neutron scattering Sternlieb *et al.*[4] predicted the Jahn-Teller distortions to be of breathing type, where all Mn-O bond lengths expand from their high temperature values. However, later theoretical calculations[6] and x-ray scattering experiments[3] found the distortions to be shear type, with longer Mn-O bonds along the ferromagnetic chain and shorter ones perpendicular to it (called type 1 henceforth) as in Fig. 2(a). In contrast, single crystal neutron diffraction data[5] supported the opposite kind of distortions: short bonds along the chain and long bonds perpendicular to it (type 2) as shown in Fig. 2(b).

Turning now to the orbital order, it was believed to be $x^2 - 1/y^2 - 1$ (rod-type) at the Mn^{3+} site by earlier studies,[3,6] while subsequent x-ray absorption[7] and resonant x-ray scattering[8] measurements supported the $x^2 - z^2/y^2 - z^2$ (cross-type) ordering (Fig. 3). Hartree-Fock calculations[9] also found the cross-type ordering to be preferred under certain octahedral distortions. But, soft x-ray resonant diffraction measurements along with cluster many-body calculations[10] found the rod-type ordering fits experiments better, which is also supported by more recent x-ray absorption and density functional theory (DFT) based calculations.[11] In a recent paper, using a model Hamiltonian, Sboychakov *et al.*[12] found that a noncubic crystal field, originating from higher neighbors in the crystal, can affect the orbital order quite strongly and in principle produce a different orbital orientation than what the local JT distortion might suggest based on the isolated octahedron physics.

The role of the Coulomb correlation on the orbital order has also been a topic of discussion. The earlier DFT calculations[6] that predicted rod-type orbital order have been criticized by Huang *et al.*[7] for not including the Coulomb correlation effects, who found that within the LDA + U or Hartree-Fock methods, a cross-type orbital order emerges. However, similar LDA + U calculations by Wu *et al.*[11] found the opposite, viz., that the rod-type orbital order is favored irrespective of the magnitude of U. Thus the role of the Coulomb interaction in determining the orbital order and also the mechanism for stabilizing the rod-type orbital order remains unclear and controversial.

To address these questions we report the results of our exact diagonalization and density-functional (DFT) studies. Our key results may be summarized as follows: (i) The density-functional calculations with full structural optimization yields

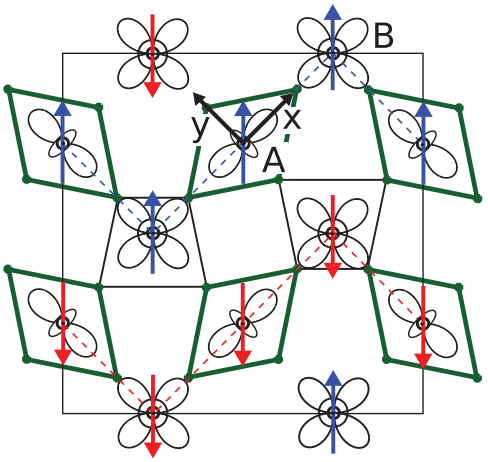

FIG. 1. (Color online) Sketch of the orbital order and Jahn-Teller distortions obtained from our studies for $La_{0.5}Sr_{1.5}MnO_4$ in the magnetic unit cell with the CE structure. The arrows represent the magnetic moments of the t_{2g} states. The Mn atoms at the bridge site (A) are nominally Mn^{3+} and those at the corner site (B) are Mn^{4+}. As shown, the bridge site has the rod-type orbital order and type 1 Jahn-Teller distortion, as obtained from our calculations and inferred from several experiments. Our DFT structural optimization yields the in-plane bridge-site Mn-O bond lengths to be $d_L = 2.06$ Å and $d_S = 1.92$ Å, and the out-of-plane bond length to be $d_O = 2.01$ Å.

a type 1 JT distortion, with elongated Mn-O bonds along the chain direction, as well as the $x^2 - 1/y^2 - 1$ (rod-type) orbital order. (ii) We find that the key physics may be described by an electronic Hamiltonian on a single ferromagnetic zigzag chain, which we study by exact diagonalization. (iii) The exact diagonalization results show the relative unimportance of the Coulomb correlation due to the low band filling (one half electron per site in the Mn $e_g \uparrow$ bands, i.e., quarter filling) and yield the rod-type orbital order, consistent with the DFT results. (iv) We find the rod-type orbital order to be favored by a strong kinetic energy term due to hopping along the zigzag chain. (v) Finally, we find from DFT calculations that a significant noncubic crystal field proposed in Ref. 12 exists, which further stabilizes the rod-type orbital order.

II. DENSITY FUNCTIONAL STUDIES

Crystal Structure—$La_{0.5}Sr_{1.5}MnO_4$ is a layered manganite that crystallizes in the orthorhombic space group $I4/mmm$ with two MnO_2 layers per unit cell.[13] The competition between hopping of e_g electrons and superexchange between the manganese t_{2g} core spins, combined with the orbital degeneracy leads to the formation of the magnetic CE phase: a checkerboard arrangement of formally Mn^{3+} $(t_{2g}^3 e_g^1)$ and Mn^{4+} $(t_{eg}^3 e_g^0)$ ions, with Mn^{3+} (A site) being JT active. Since not all orbitals are fully occupied, this also leads to an orbital-polarized ground state. The two hotly debated candidates for the orbitally ordered state in this system are shown in Figs. 3(a) and 3(b). The structures differ in the occupied e_g orbital at the Mn^{3+} site which has either the rod-type $(x^2 - 1/y^2 - 1)$ ordering or the cross-type $(x^2 - z^2/y^2 - z^2)$ ordering. In both cases, Mn^{4+} (B site) atoms are made up of nominally empty e_g orbitals and are not JT active.

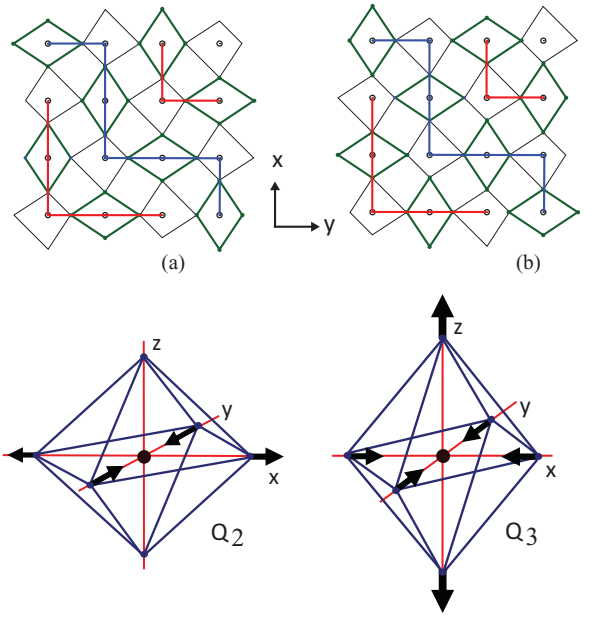

FIG. 2. (Color online) Two kinds of lattice distortions in the *ab* plane containing the zigzag chains, depending on whether Mn-O bond lengths along the chain direction (a) elongate (type 1) or (b) compress (type 2). Green lines indicate the octahedra around A sites and black lines indicate those around B sites. In both cases, the out of plane Mn-O distance is about 2 Å and is close to the longer in-plane Mn-O bond length. The normal modes Q_2 and Q_3 of the MnO_6 octahedron are shown in the bottom part. Referring to the particular JT atom, labeled by A in Fig. 1, the type 1 distortion corresponds to $Q_2 > 0$, while type 2 corresponds to $Q_2 < 0$. The signs of Q_2 alternate between positive and negative between consecutive bridge-site atoms on the zigzag chain.

DFT Method—First-principles density functional theory calculations were performed using the Vienna *ab initio* simulation package,[14,15] within the projector augmented wave method. We used the generalized gradient approximation (GGA)[16] with a plane wave energy cutoff of 450 eV and k-space sampling on a $4 \times 4 \times 4$ Monkhorst-Pack grid. All structural relaxations were carried out till Hellman-Feynman forces became less than 0.01 eV/Å. To study $La_{0.5}Sr_{1.5}MnO_4$, a simulation cell $4 \times 4 \times 1$ times the crystallographic unit cell was used, containing 16 molecules of Sr_2MnO_4 doped with 1/2 electron per molecule. A uniform positive background makes the supercell neutral. The additional electrons reside at the Mn^{3+} sites as expected. We also repeated the calculations using virtual atoms with valence atomic number 10.25 $(0.25Z_{La} + 0.75Z_{Sr})$ with the QUANTUM-ESPRESSO package.[17] In both calculations the main results remained unchanged. We also repeated our calculations with an onsite repulsion term with the GGA + U method, which was suggested to affect the orbital ordering.[7] However, for reasonable values of U (5 eV) at Mn-d site, we find our conclusions to be qualitatively unchanged. This is expected, because the e_g states are sparsely occupied (1/2 electron per site), so that the Coulomb correlation is weaker, a result that was further confirmed from the exact diagonalization calculations for a zigzag chain as discussed later.

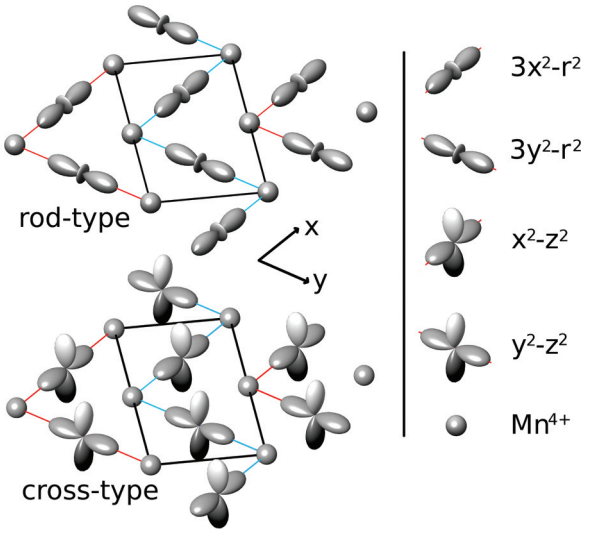

FIG. 3. (Color online) Two types of orbital ordering in the MnO_2 plane (oxygen atoms are not shown) of $La_{0.5}Sr_{1.5}MnO_4$: rod-type $(x^2 - 1/y^2 - 1)$ and cross-type $(x^2 - z^2/y^2 - z^2)$. The crystallographic unit cell boundary is marked by black lines. The ferromagnetic zigzag chains in this so-called CE structure alternate between spin-up (red lines) and spin-down (blue lines) chains.

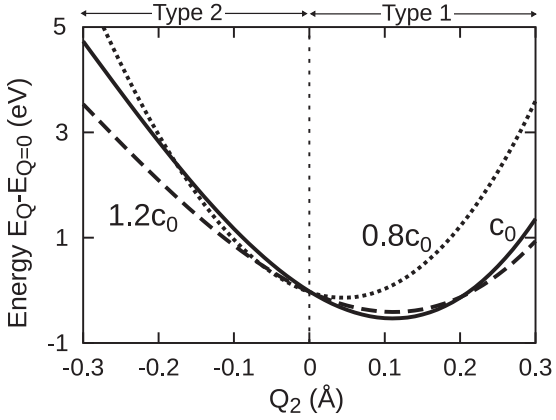

FIG. 4. Variation of the total energy as a function of the JT distortion Q_2 with unstretched (c_0 corresponding to $Q_3 = 0.12$ Å), stretched ($1.2c_0$ or $Q_3 = 0.54$ Å) and compressed ($0.8c_0$ or $Q_3 = -0.40$ Å) unit cells along the c axis. The volume was relaxed in each case keeping the Q_2 and Q_3 fixed (or a fixed c axis length). The minimum always occurred at a positive Q_2 along with the rod-type orbital order, so that the strain along the c axis does not have any significant effect on the JT distortion or the orbital order.

Results—For the structural optimization we started with the undistorted structure with the experimental lattice parameters and performed a global optimization of the ionic coordinates and the cell parameters. The relaxed volume was found to be $V_0 = 98.5$ Å^3 per formula unit (f.u.) which is higher than the experimental value of 92.6 Å^3/f.u.[13] as expected from GGA calculations. The lattice parameters for the relaxed structure are $a = b = 11.2$ Å and $c = 12.6$ Å. We fixed this volume for all subsequent calculations at the calculated value V_0.

When the ionic positions are relaxed, we find the oxygen octahedra around the Mn^{3+} site to undergo a JT distortion. The resultant distortions are of type 1, as shown in Fig. 2(a) with the Mn-O bond lengths elongated along the zigzag chain direction. The calculated in-plane bond lengths are $d_L = 2.06$ Å along the chain direction and $d_S = 1.92$ Å perpendicular to the chain, while the out-of-plane bond length is $d_O = 2.01$ Å.

The Q_3 mode describes the stretching (for $Q_3 > 0$) of the MnO_6 octahedron in the z direction along with the compression in the x and y directions, while Q_2 mode describes the stretching (for $Q_2 > 0$) in the x direction and compression in the y direction of the octahedron as shown in the lower panel of Fig. 2. In both cases the volume of the octahedron does not change. Together they can represent the experimentally debated JT distortion in this system. In terms of the out-of-plane Mn-O bond length (d_O) and in-plane long (d_L) and short (d_S) Mn-O bonds, we can write $Q_2 = d_L - d_S$ and $Q_3 = \frac{1}{\sqrt{3}}[2d_O - (d_L + d_S)]$. In the case of Fig. 2(a), the longest in-plane bond length d_L is along the direction connecting ferromagnetic Mn, while for Fig. 2(b) it is perpendicular to the chain. Our calculated bond lengths from the DFT optimization mentioned above corresponds to the JT distortions of $Q_2 = 0.14$ Å and $Q_3 = 0.02$ Å, so that the net magnitude is $Q \equiv \sqrt{Q_2^2 + Q_3^2} = 0.14$ Å.

Note that due to the zigzag nature of the ferromagnetic chain, the sign of the Q_2 mode alternates between successive A sites on the chain, while the orbital order alternates between $x^2 - 1$ and $y^2 - 1$ as indicated from Figs. 2 and 3. For clarity of discussion we concentrate on one of the Mn atoms: The site marked as A in Fig. 1 where the type 1 distortion corresponds to a positive Q_2 and the rod-type orbital ordering corresponds to the $|x^2 - 1\rangle$ orbital.

To study the energetics of the proposed type 2 structure of Refs. 5 and 11, with the JT distortion $Q_2 = -0.09$ and $Q_3 = 0.06$ Å, we computed its total energy, which came out to be higher by about 110 meV/Mn. Upon relaxation this structure also deformed to the configuration obtained in our previous calculation, viz., to the type 1 structure, confirming that the latter structure is more stable.

We find that the type of the JT distortion as well as the orbital order are quite robust and largely unaffected by a strain along the c axis. The calculated energy as a function of the in-plane distortion Q_2 (with fixed Q_3, which is directly related to the c-axis strain) is shown in Fig. 4. For the unstrained structure corresponding to $Q_3 = 0.12$ Å, the minimum in energy is at $Q_2 = 0.14$ Å. Elongation of the c axis ($Q_3 = 0.54$ Å) makes the minimum shallower but does not alter its position, while compression ($Q_3 = -0.4$ Å) moves it closer to $Q_2 = 0$ but the minimum still remains on the positive side. The orbital order corresponding to the energy minimum was also found to be the rod type in each of the cases. Thus the JT distortion as well as the orbital order are both robust and do not change significantly with the external strain.

The calculated DFT band structure is consistent with the nominal chemical valence Mn^{3+} $(t_{2g}^3\uparrow e_g^1\uparrow)$ for the A site and Mn^{4+} $(t_{2g}^3\uparrow)$ for the B site, although the charge disproportionation is much weaker than what these nominal valences would suggest. In fact, the density of states for the occupied majority-spin $e_g\uparrow$ states, shown in Fig. 5, suggests a substantial Mn e_g distribution on the B site Mn atoms. A more

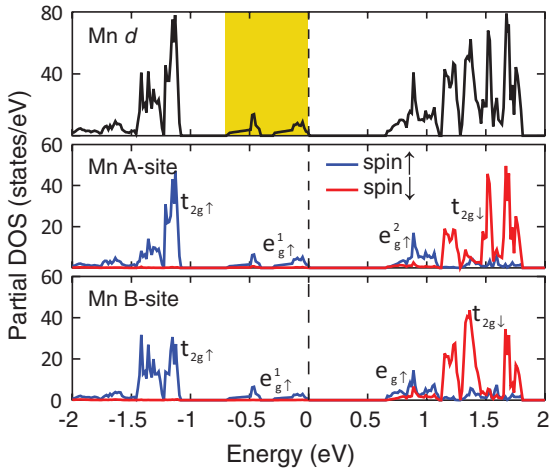

FIG. 5. (Color online) Partial Mn-d density of states/cell obtained from DFT calculations for the relaxed structure: total Mn (*top*), bridge site Mn (*middle*), and corner site Mn (*bottom*). Each Mn has the majority-spin t_{2g} orbitals fully occupied, while out of the four majority-spin e_g orbitals on the A and B sites, just one is occupied, with a significantly larger weight on the A site, leading to the nominal chemical valence Mn^{3+} ($t_{2g}^3\uparrow e_g^1\uparrow$) for the A site and Mn^{4+} ($t_{2g}^3\uparrow$) for the B site. The shaded region is the energy window used to calculate the partial charge densities in Fig. 6. Fermi level is set to 0 eV.

careful, quantitative analysis shows the distribution of the e_g electrons between the A and the B sites to be roughly 2:1,[18] so that the occupied e_g electron has the predominant A site (bridge site) character. It may be noted that GGA+U calculations will enhance this charge disproportionation (Δn), because U favor the singly occupied bridge sites, as can be seen from our exact diagonalization results presented in Fig. 9. In Fig. 5 the $e_g^1\uparrow$ is further split into two peaks due to hybridization between the two Mn sites on the zigzag chain.

To understand the orbital ordering, the charge density $\rho(r) = \int_{\epsilon_1}^{\epsilon_2} |\psi(r,\epsilon)|^2 d\epsilon$ was computed by integration over the energy window spanning the occupied e_g states as indicated in Fig. 5. The results shown in Fig. 6 indicate that the orbital order at the bridge site is rod type and that this does not change whether we have a relaxed or unrelaxed structure. The charge density isosurfaces at the bridge sites are clearly seen to have the $|z^2 - 1\rangle$ symmetry with the z axis pointed along the zigzag chain, while the surfaces at the corner sites are made of a superposition of both e_g orbitals. The figure also shows the hybridization of the e_g states with the in-plane oxygen atoms. The orbital order remains more or less the same in the relaxed structure which has a much stronger JT distortion as compared to the unrelaxed structure. In fact, Fig. 7 shows that the rod-type orbital order is preferred over the cross-type order irrespective of the JT distortion. As confirmed from the model studies presented below, it is the kinetic energy term that favors the rod-type order, which is largely unaffected by the distortion of the oxygen octahedra found around the bridge site.

III. TIGHT-BINDING MODEL

To understand the competition between the orbital orientation and the JT distortion, we consider the minimal model

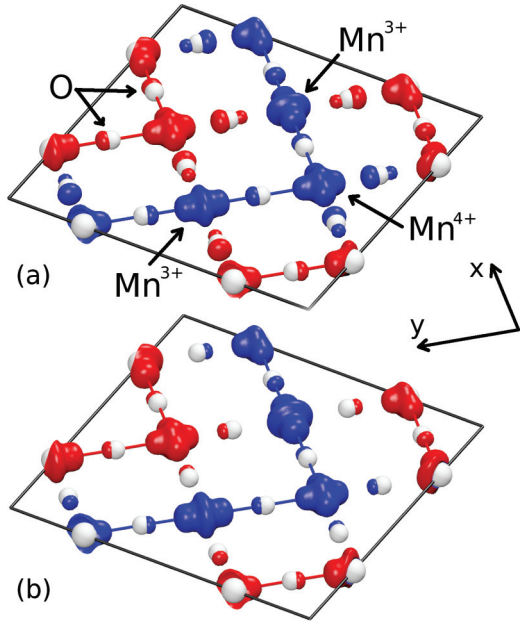

FIG. 6. (Color online) Charge density contours for the occupied e_g states on the ab plane obtained from the DFT calculations for the unrelaxed structure (*top*) with ($Q_2 = 0$ and $Q_3 = 0.12$ Å) and relaxed structure (*bottom*) with ($Q_2 = 0.14$ and $Q_3 = 0.02$ Å). The orbital ordering remains more or less unchanged by the JT distortion. Blue and red isosurfaces correspond, respectively, to spin-up and spin-down charge densities of magnitude 0.057 e^-/eV. Ferromagnetic zigzag chains are indicated by the colored lines.

of a single ferromagnetic zigzag chain of Mn atoms, which is well known to describe the basic physics in the half-doped manganite materials with CE magnetic structure.[12,18] Since

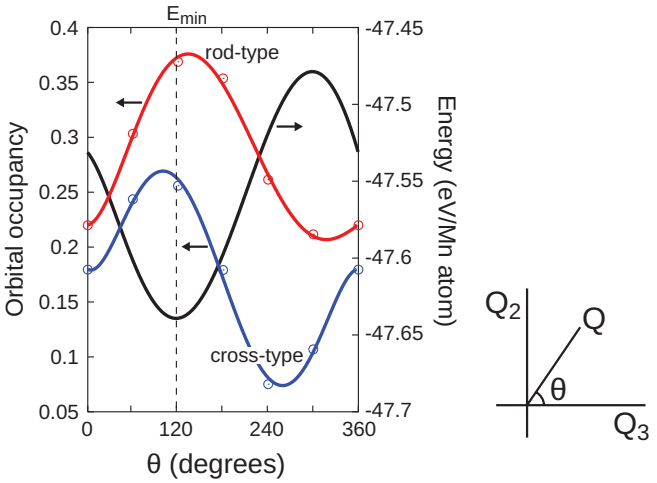

FIG. 7. (Color online) Change of orbital occupancy of the bridge-site atom with JT distortion and the corresponding total energy as obtained from the density-functional calculations. The rod-type orbital order is preferred over the cross-type order irrespective of the JT distortion angle $\theta \equiv \tan^{-1}(Q_2/Q_3)$. The vertical dashed line corresponds to the minimum energy structure, which has the rod-type orbital order and the type 1 JT distortion ($\theta \approx 90^\circ$). Notice the similarity of the results with Fig. 8, which reveals the effect of the noncubic crystal field in stabilizing the rod-type orbital order.

the double exchange prevents electronic hopping between the zigzag chains, owing to the antiferromagnetic order between the neighboring chains, the essential physics may be described by considering the Hamiltonian for a single zigzag chain of Mn e_g orbitals. We consider the Hamiltonian

$$\mathcal{H} = \mathcal{H}_{\rm ke} + \sum_k \left(\mathcal{H}^k_{\rm JT} + \mathcal{H}^k_{\rm NC}\right) + \sum_k \left(\frac{1}{2} K Q_k^2 - \lambda Q_{3k}\right) + \mathcal{H}_{\rm U}, \quad (1)$$

where the various terms are, respectively, the kinetic energy, the JT interaction, a noncubic crystal field arising out of second and higher neighbor interactions, the isotropic elastic energy term $1/2KQ^2$, an anisotropic elastic energy term characterized by λ that shifts the equilibrium away from the origin (in this case to a nonzero Q_3), and finally an on-site Coulomb interaction between the electrons. The anisotropic elastic energy term takes care of the fact that the out-of-plane oxygens are connected to a different type of ion (La/Sr) unlike the in-plane oxygens that interlink Mn, which leads to an elongation of out-of-plane Mn-O bond length ($\lambda > 0$). All these terms are standard in the literature except that we have introduced the noncubic crystal field term $\mathcal{H}_{\rm NC}$ following the work of Sboychakov and co-workers,[12] and the anisotropic elastic energy term, both arising from the fact that the planar *ab* directions are significantly different from the *c* direction. This leads to the splitting of e_g bands even in the absence of any JT distortions and justifies adding a tetragonal component to the cubic crystal field, both to the orbital energy as well as to the elastic energy term.

The kinetic energy term in the Hamiltonian is given by

$$\mathcal{H}_{\rm ke} = \sum_{\langle ij\rangle,\sigma} \sum_{\alpha\beta} V_{ij}^{\alpha\beta} c^\dagger_{i\alpha\sigma} c_{j\beta\sigma} + \text{H.c.} - J_H \sum_{i\alpha} S_i \cdot \sigma_{i\alpha}, \quad (2)$$

where $c^\dagger_{i\alpha\sigma}$ creates an e_g electron at site i, with spin σ and orbital index α. The t_{2g} core spins S are considered classical and in the limit of strong Hund's coupling $J_H = \infty$, which we have used here, we cannot only ignore the electron hopping between neighboring antiferromagnetic chains, but also just one spin state, the one parallel to the t_{2g} core spins S, is relevant for modeling the e_g electrons on the ferromagnetic zigzag chain. In the basis $|z^2 - 1\rangle$ and $|x^2 - y^2\rangle$, the hopping integral V has the form for NN interactions

$$V^{\alpha\beta} = \begin{pmatrix} 1 & \pm\sqrt{3} \\ \pm\sqrt{3} & 3 \end{pmatrix} \times \frac{V_{dd\sigma}}{4},$$

where the minus (plus) sign corresponds to the hopping in the $x(y)$ direction. The JT coupling at each site is given by[19–22]

$$H_{\rm JT} = g(Q_2\tau_x - Q_3\tau_z), \quad (3)$$

where only the linear JT coupling term has been included, the quadratic coupling term $-G[(Q_3^2 - Q_2^2)\tau_z + 2Q_2Q_3\tau_x]$ is too small to change the essential physics presented here, and $\vec{\tau}$ is the pseudospin describing the two e_g orbitals: $|\uparrow\rangle = |z^2 - 1\rangle$ and $|\downarrow\rangle = |x^2 - y^2\rangle$. In Eq. (1) the sum k runs over all JT active (Mn^{3+}) sites and $Q_k^2 = Q_{1k}^2 + Q_{2k}^2 + Q_{3k}^2$. The Coulomb interaction term contains the on-site Coulomb repulsion, so that

$$\mathcal{H}_{\rm U} = U \sum_{k\alpha\beta}{}' n_{k\alpha\sigma} n_{k\beta\sigma}, \quad (4)$$

where the prime on the summation excludes the self-interaction $\alpha \neq \beta$ and as we have mentioned earlier only one spin state σ parallel to the t_{2g} spins of the ferromagnetic zigzag chain needs be considered.

The noncubic crystal field has the form $\mathcal{H}_{\rm NC} = \Delta\tau_z$, which splits the two e_g states further beyond the JT splitting term. We have estimated the strength Δ of this field from our DFT calculations. In the undistorted structure structure with volume V_0, all in-plane Mn-O distances are equal, $d_{\rm L} = d_{\rm S} = 1.98$ Å, while the out-of-plane Mn-O bond lengths are already elongated to $d_{\rm O} = 2.04$ Å due to the asymmetry in bonding. This corresponds to a $Q_3 = 0.12$ Å and zero in-plane JT distortion $Q_2 = 0$. Ignoring the hopping between the orbitals, this splitting is caused by the JT distortions and the crystal field parameter Δ through the on-site part of the Hamiltonian, which for $Q_2 = 0$ becomes $E = (-gQ_3 + \Delta)\tau_z$. In the DFT results, the $|x^2 - y^2\rangle$ state at the A-site Mn ions is split below $|z^2 - 1\rangle$ by the amount $\delta E = 0.6$ eV. With $Q_3 = 0.12$ Å and taking the typical range for $g = 1.5$–2.0 eV/Å,[20] we find that $\Delta = 0.48$–0.54 eV. It is difficult to isolate the anisotropic elastic energy parameter λ from the DFT calculations. The estimated value is $\lambda \sim 1$ eV, which we have obtained by comparing the total energies between the model Hamiltonian and the DFT results.

We solve the model Hamiltonian Eq. (1) by exact diagonalization on a finite-size chain. In this method the ground state is expanded in terms of the many-particle configurations $|i\rangle$: $|G\rangle = \alpha_i|i\rangle$, and the resulting Hamiltonian matrix is diagonalized using the Lanczos method. We considered a 12-site zigzag chain of Mn atoms with periodic boundary conditions. A second method is to solve the Hamiltonian for the infinite chain by obtaining the tight-binding band structure, but in this case some mean-field approximation such as the Hartree approximation ($\mathcal{H}_{\rm U} \approx U \sum'_{k\alpha\beta} \langle n_{k\alpha}\rangle n_{k\beta} + n_{k\alpha}\langle n_{k\beta}\rangle - \langle n_{k\alpha}\rangle\langle n_{k\beta}\rangle$) must be made for the interaction term.

Our analysis shows that the kinetic energy involving electron hopping along the ferromagnetic chain is an important factor for the rod-type orbital ordering. This can be easily seen by solving the band structure for the Hamiltonian $\mathcal{H}_{ke}$ [Eq. (2)], which yields the eigenvalues $\pm\frac{1}{2}\sqrt{8t^2 + 4t^2\cos k_x a}$ (where k_x is the Bloch momentum along the chain) and the corresponding eigenvectors consist of predominantly rod-type orbitals at the Mn^{3+} site.[18] Summing over the occupied states, we find that the orbital occupancy of the rod-type orbital $(x^2 - 1)$ is as much as 75%, while the remaining 25% is occupied by the other e_g orbital, viz., $y^2 - z^2$, indicating the preference for the rod-type order by the kinetic energy term.

The JT interaction can affect the above orbital order by preferring one orbital over the other by modifying the on-site orbital energies. This is illustrated by calculating the orbital occupancies as a function of the JT distortion type, parametrized by the angle θ ($Q_2 = Q\sin\theta$ and $Q_3 = Q\cos\theta$), which can be calculated from either the exact diagonalization or the tight-binding method. The results obtained from these methods are similar and we have shown the results from the former

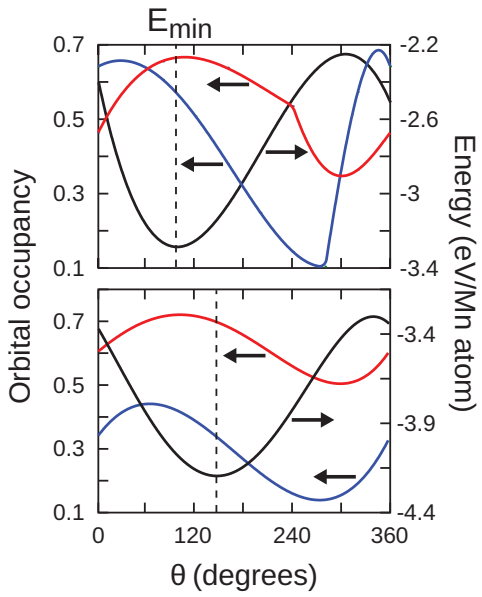

FIG. 8. (Color online) ED results for the orbital occupancies of the bridge site Mn atom and the total energy. Shown are the rod-type $x^2 - 1$ (red) and the cross-type $x^2 - z^2$ (blue) orbital occupancies as well as the total energy as a function of the JT distortion angle with a noncubic crystal field $\Delta = 0$ (top) and $\Delta = 0.5$ eV (bottom). Parameters are: $V_{dd\sigma} = -0.5$ eV and $g = 1.5$ eV/Å. Also $\lambda = 1$ eV in the bottom figure. Since the magnitude of the JT distortion Q is fixed in this figure, the elastic term $1/2KQ^2$ merely adds a constant shift to the energy.

method in Fig. 8. In the figure we have shown the occupancies of the rod-type and the cross-type orbitals as a function of the JT distortion angle. The top figure shows that the rod-type order is generally favored, but for some values of θ, the cross-type order is favored. The minimum energy structure has nevertheless the rod-type order. The bottom figure, where we have added a noncubic crystal field ($\Delta = 0.5$ eV), indicates that the rod-type ordering is considerably stabilized by the noncubic crystal field. Notice the similarity of these results with those obtained from the density functional calculations shown earlier in Fig. 7.

In order to illustrate the relative unimportance of the Coulomb interaction effects on the charge and orbital ordering, we have carried out the exact diagonalization calculations with $U = 0$ and 5 eV. The Coulomb effects are not expected to be very important because the relevant e_g bands are only quarter filled (only half electron per Mn site to fill the two majority-spin e_g orbitals). The results are shown in Fig. 9, where we have defined the charge order parameter as $\Delta n \equiv n_A - n_B$, A and B being the bridge-site and the corner-site Mn atoms, and the orbital order parameters as $\eta_A \equiv n_{A1} - n_{A2}$ and $\eta_B \equiv n_{B1} - n_{B2}$, with $|A1\rangle = x^2 - 1$ and $|A2\rangle = y^2 - z^2$, and similarly for the B atoms. The figure confirms the charge disproportionation similar to Mn^{3+} and Mn^{4+} as well as the rod-type order at the A site and additionally the relative unimportance of the Coulomb interaction term, all as anticipated.

In order to study the energy landscape in the Q_2-Q_3 plane, we have computed the total energy by calculating the tight-binding band structure for the infinite zigzag chain from the

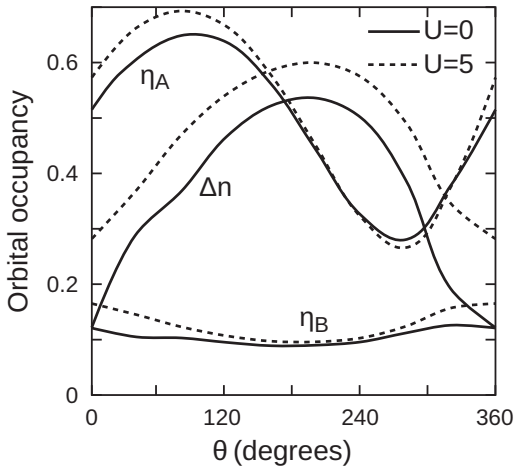

FIG. 9. ED results for the charge orbital order for the bridge site and the corner site atoms as a function of the JT distortion angle. The results indicate the predominant occupation of the rod-type orbital at the A site as well as the charge disproportionation $\Delta n \equiv n_A - n_B$ consistent with the nominal valences of Mn^{3+} and Mn^{4+} for the two types of Mn atoms, although the charge disproportionation is significantly smaller than one, a result that is also found from the DFT results.

Hamiltonian Eq. (1). The results are shown as a contour plot in Fig. 10 for typical values for the parameters. The previously reported values[5,7,11] of the JT distortion are also indicated in the figure. Following the convention mentioned previously, the minimum on the positive Q_2 axis at (0.2,0.06)Å corresponds to Fig. 2(a) or type 1 distortion. The type 1 structure is considerably lower in energy than the type 2 structure, by about 0.43 eV, which strongly suggests the type 1 JT distortion to be the preferred ground state, consistent with the DFT results discussed in the previous section.

From the tight-binding wave functions, the nature of the orbital ordering can be studied by summing the orbital

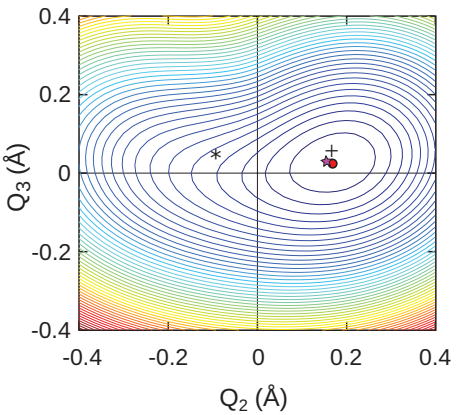

FIG. 10. (Color online) Total energy contours for the tight-binding model in Eq. (1) on the (Q_2, Q_3) plane. The tight-binding minimum-energy structure is marked by the red dot, the star is our DFT result discussed in the previous section, while the "+" and "*" symbols correspond to the previously reported values in Refs. 5 and 7, respectively. Our calculations support type 1 kind of distortion. Parameters used are $V_{dd\sigma} = -0.5$ eV, $g = 1.5$ eV/Å, $K = 10$ eV/Å^2, $\lambda = 1$ eV/Å, $U = 0$, and $\Delta = 0.5$ eV.

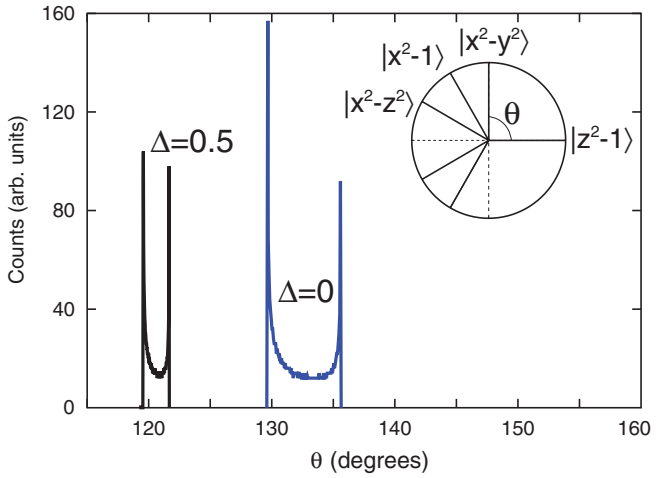

FIG. 11. (Color online) Histogram plots showing distribution of angles corresponding to basis occupancies for different values of second neighbor crystal field parameter Δ. Value of 120° corresponds to $|x^2 - 1\rangle$ (rod type), whereas 150° corresponds to $|x^2 - z^2\rangle$ (cross type) as shown in the inset.

components of the wave functions over the occupied part of the Brillouin zone. The e_g wave function at any k point can be written as the linear combination $|\Psi_k\rangle = \cos\theta_k|z^2 - 1\rangle + \sin\theta_k|x^2 - y^2\rangle$, so that the rod-type orbital $|x^2 - 1\rangle$ corresponds to $\theta_k = 120°$, while the cross-type orbital $|x^2 - z^2\rangle$ corresponds to $\theta_k = 150°$. Figure 11 show the histogram of the θ_k for the minimum-energy structures with the same parameters as in Fig. 10 for two values of the noncubic crystal field Δ. For $\Delta = 0.5$ eV, the histogram indicates that the values of θ_k are bunched around $\theta_k = 120°$, indicating a clear rodlike orbital order, while in the absence of a crystal field ($\Delta = 0$), the values of θ_k lie in the region of $\theta \sim 130°$–$135°$, which is in between the rodlike and the crosslike orbital order, but more like the former. The results again show that the rodlike orbital order is further strengthened by the noncubic crystal field.

IV. CONCLUSION

In conclusion, we have studied the orbital ordering and the Jahn-Teller distortion in $La_{0.5}Sr_{1.5}MnO_4$ from density-functional studies and evaluated the origin of this ordering from model studies using exact diagonalization and tight-binding band structure methods. The density-functional calculations including a global minimization of the structural parameters show a type 1 JT distortion and a rod-type orbital ordering. The shear-type JT distortion was correctly concluded from the x-ray measurements in Ref. 3, but is different from the distortions suggested from the other experiments.[4,5] The rod-type orbital order is in agreement with the x-ray scattering measurements as well as an earlier theoretical study, but is different from the cross-type order suggested in Refs. 8 and 9. Exact diagonalization and tight-binding model studies allowed us to examine the interplay between the various energy terms and revealed the reason for the particular orbital order. It was shown that the electronic hopping along the zigzag chain is an important factor in determining the orbital order, while a noncubic crystal field, of the type proposed earlier by Sboychakov *et al.*,[12] further strengthens the occupation of the rod-type orbital. The type 1 JT distortion was found to be the minimum-energy structure, with elongated Mn-O bond lengths along the zigzag chain and compressed bond lengths perpendicular to it, which is just what would be expected for the isolated MnO_6 octahedron. Our work provides important insights into the effects of the various competing terms in determining the cooperative Jahn-Teller and orbital ordering in the crystalline environment, where terms such as electronic hopping, noncubic crystal fields, electron correlations, and anisotropic elastic energy, all could play important roles.

ACKNOWLEDGMENT

This work was supported by the Office of Basic Energy Sciences of the US Department of Energy through Grant No. DE-FG02-00ER45818.

*Permanent address: High Pressure, and Synchrotron Radiation Physics Division, Bhabha Atomic Research Centre, Mumbai 400085, India; shanavasv@missouri.edu

[1] Y. Tokura, Science **288**, 462 (2000).
[2] E. Dagotto, *Nanoscale Phase Separation and Colossal Magnetoresistance: The Physics of Manganites and Related Compounds* (Springer, Berlin, 2003).
[3] S. Larochelle, A. Mehta, N. Kaneko, P. K. Mang, A. F. Panchula, L. Zhou, J. Arthur, and M. Greven, Phys. Rev. Lett. **87**, 095502 (2001).
[4] B. J. Sternlieb, J. P. Hill, U. C. Wildgruber, G. M. Luke, B. Nachumi, Y. Moritomo, and Y. Tokura, Phys. Rev. Lett. **76**, 2169 (1996).
[5] O. Schumann, Ph.D. thesis, University of Cologne, 2010.
[6] P. Mahadevan, K. Terakura, and D. D. Sarma, Phys. Rev. Lett. **87**, 066404 (2001).
[7] D. Huang, W. Wu, G. Guo, H.-J. Lin, T. Hou, C. Chang, C. Chen, A. Fujimori, T. Kimura, H. Huang *et al.*, Phys. Rev. Lett. **92**, 087202 (2004).
[8] S. B. Wilkins, N. Stojić, T. A. W. Beale, N. Binggeli, C. W. M. Castleton, P. Bencok, D. Prabhakaran, A. T. Boothroyd, P. D. Hatton, and M. Altarelli, Phys. Rev. B **71**, 245102 (2005).
[9] K. Ebata, T. Mizokawa, and A. Fujimori, Phys. Rev. B **72**, 233104 (2005).
[10] A. Mirone, S. S. Dhesi, and G. van der Laan, Eur. Phys. J. B **53**, 23 (2006).
[11] H. Wu, C. Chang, O. Schumann, Z. Hu, J. Cezar, T. Burnus, N. Hollmann, N. Brookes, A. Tanaka, M. Braden *et al.*, Phys. Rev. B **84**, 155126 (2011).
[12] A. O. Sboychakov, K. I. Kugel, A. L. Rakhmanov, and D. I. Khomskii, Phys. Rev. B **83**, 205123 (2011).
[13] C. S. Hong, E. O. Chi, W. S. Kim, N. H. Hur, K. W. Lee, and C. H. Lee, Chem. Mater. **13**, 945 (2001).
[14] G. Kresse and J. Hafner, Phys. Rev. B **47**, 558 (1993).
[15] G. Kresse and J. Furthmuller, Phys. Rev. B **54**, 11169 (1996).
[16] J. P. Perdew, K. Burke, and M. Ernzerhof, Phys. Rev. Lett. **77**, 3865 (1996).

[17]P. Giannozzi, S. Baroni, N. Bonini, M. Calandra, R. Car, C. Cavazzoni, D. Ceresoli, G. L. Chiarotti, M. Cococcioni, I. Dabo *et al.*, J. Phys.: Condens. Matter **21**, 395502 (2009).
[18]Z. Popović and S. Satpathy, Phys. Rev. Lett. **88**, 197201 (2002).
[19]I. Bersuker, *The Jahn-Teller Effect* (Cambridge University Press, Cambridge, 2006).
[20]Z. Popović and S. Satpathy, Phys. Rev. Lett. **84**, 1603 (2000).
[21]B. R. K. Nanda and S. Satpathy, Phys. Rev. B **81**, 174423 (2010).
[22]Note that the convention for the JT distortion mode Q_2 in this paper is negative of the same quantity defined in Refs. 20 and 21.